J. Indian Inst. Sci., May–June 1991, 71, 283–311.

IISc THESES ABSTRACTS

Thesis Abstract (Ph.D.)

Ergodic and adaptive control of Markov processes* by Mrinal Kanti Ghosh.
Research supervisors: V. S. Borkar and V. G. Tikekar.
Department: Applied Mathematics.

1. Introduction

We address a few questions in stochastic control theory which still elude completely satisfactory answers. We consider dynamical systems that evolve over time according to some probabilistic law of motion satisfying the Markovian assumption. The probabilistic law of motion can be controlled by taking decisions, *i.e.*, choosing a suitable element from a set, called the control set.

In the first type of problems we treat, the decision maker (controller) has the complete information of the past and present but no anticipation of the furture is allowed. Also costs are incurred and as a consequence of which instantaneous decisions are taken as the system evolves over time. An infinite planning horizon is assumed and the goal is to find an aggregate of decision (policy) so as to minimize the 'ergodic' or 'long-run average cost' criterion. We show that there is a definitive way of finding a choice which attains the minimum possible value for this criterion.

After making a tour in the realm of ergodic control, we venture to enter a more rugged terrain where uncertainty prevails in an essential way. The structure of the system is not completely known to the decision maker due to the involvement of an unknown parameter. This is the so-called adaptive control problem and is of paramount importance in the practical domains. We assume that the model set is prescribed in a parametric form and then implement an *ad hoc* separation between estimation and control aspects in the following manner: At each time, the control used is the one which would have been optimal choice if the current parameter estimate, obtained by some on-line scheme, were the true parameter. This is the so-called self-tuning scheme. We develop a self-tuning regulator for our purpose and establish its asymptotic optimality.

While studying the asymptotics of controlled Markov processes in the context of ergodic or adaptive control, we confine our attention to two important classes of Markov processes, *viz.*, Markov chains and diffusion processes.

2. Model description and results

2.1. *Controlled Markov chains*

Let $\{X_n\}$ be a controlled Markov chain with state space $S = \{0, 1, 2, \ldots\}$, action space A, any compact metric space. A control strategy or policy is any rule for choosing actions based on past observations.

*This work was carried out under the TIFR–IISc Programme in Applications of Mathematics.

A stationary policy is a function $f: S \to A$. If the chain is ergodic under a stationary policy it is called a stable stationary policy. If X_n denotes the state of the process at time n and u_n the action chosen at n, under some policy, we denote

$$p(i,j,u) = P(X_{n+1} = j | X_0, u_0, \ldots, X_n = i, u_n = u).$$

Let $k: S \times A \to \mathbb{R}$ be the cost function. Our objective is to *a.s.* minimize

$$\liminf_{N \to \infty} \frac{1}{N} \sum_{n=0}^{N-1} k(X_n, u_n)$$

over all policies. If the minimum is obtained for a policy, it is called an optimal policy. It has been shown[1] by direct methods that under a certain condition on the cost function for penalizing unstable behaviour or under some blanket stability condition, optimal stable stationary policies exist and can be characterized *via* dynamic programming. Here (see Borkar[2]) we use the conventional 'vanishing discount' approach, *i.e.*, first treat the related discounted cost criterion, *viz.*, minimize overall policies

$$E\left[\sum_{n=0}^{\infty} \beta^n k(X_n, u_n)\right], \quad 0 < \beta < 1$$

and then study the limiting case as $\beta \to 1$ to derive the results for the average cost criterion. This approach has the advantage that similar arguments can be used to derive the results for adaptive control which we describe below.

We consider the non-Bayesian adaptive control of Markov chains. The transition probabilities $p(i,j,u,\theta)$ now depend on an unknown parameter $\theta \varepsilon D$, D a compact metric space, the 'true' value of which is $\theta_0 \varepsilon D$. The cost criterion is again 'long-run average cost'. A direct approach to minimization is not possible as the structure of the system is not completely known. We develop a self-tuning regulator to treat this situation and establish its asymptotic optimality under an identifiability condition.

2.2. *Controlled diffusion processes*

We consider $\mathbb{R}^d$-valued process governed by a controlled stochastic differential equation of Ito type

$$\mathrm{d}X(t) = m(X(t), u(t))\mathrm{d}t + \sigma(X(t))\mathrm{d}W(t), X(0) = X_0$$

where $m: \mathbb{R}^d \times U \to \mathbb{R}^d$ and $\sigma: \mathbb{R}^d \to \mathbb{R}^{d \times d}$-matrix valued, are, respectively, the drift vector and diffusion matrix, $\sigma\sigma^T$ is assumed to be uniformly elliptic, $W(t)$ a standard d-dimensional Wiener process independent of X_0 (a prescribed $\mathbb{R}^d$-valued random variable), and $u(t)$ a non-anticipative control process taking values in a given compact metric space U. If $u(t) = v(X(t))$ for a measurable $v: \mathbb{R}^d \to U$, we call it a Markov control. If the process $X(t)$ is ergodic under a Markov control, it is called a stable Markov control.

Let $k: \mathbb{R}^d \times U \to \mathbb{R}$ be the cost function. We want to *a.s.* minimize

$$\liminf_{T \to \infty} \frac{1}{N} \int_0^T k(X(t), u(t))\mathrm{d}t$$

over all admissible controls. If the minimum is obtained for some control $u(\cdot)$, it is called an optimal. The existence of an optimal stable relaxed Markov control has been established[3]. Here, (see Borkar

and Ghosh[4]) we characterize the same by studying the Hamilton–Jacobi–Bellman equation for the ergodic control problem. Using this characterization we prove the existence of a stable Markov control. Again, we use the traditional 'vanishing discount' approach. For $\lambda > 0$, we first minimize

$$E\left[\int_0^\infty e^{-\lambda t} k(X(t), u(t))\mathrm{d}t\right]$$

over all admissible controls and study the case as $\lambda \to 0$. The limiting argument is heavily based on the theory of quasilinear uniformly elliptic equations.

We next treat the adaptive control of diffusion processes. Here the drift depends on an unknown parameter. As in the case of controlled Markov chains, we develop a self-tuning regulator to deal with the situation and establish its asymptotic optimality.

At the end we briefly discuss the situation when the diffusion is degenerate. We modify the methodology of Borkar and Ghosh[3] to show the existence of an optimal control for the ergodic control problem.

References

1. Borkar, V. S. — Control of Markov chains with long-run average cost criterion, in *Proc. IMA Workshop on Stochastic Differential Systems with Applications in Elec/Computer Engng, Control Theory and Operations Research* (W. Fleming and P. L. Lions, eds), 1987, pp 55–77, Springer Verlag.
2. Borkar, V. S. and Ghosh, M. K. — Ergodic and adaptive control of nearest neighbour motions, *Math. Control Signals Systems*, 1991, **4**, 81–98.
3. Borkar, V. S. and Ghosh, M. K. — Ergodic control of multi-dimensional diffusions I: The existence results, *SIAM J. Control Optimization*, 1988, **26**, 112–126.
4. Borkar, V. S. and Ghosh, M. K. — Ergodic control of multi-dimensional diffusions II: Adaptive control, *Appl. Math. Optimization*, 1990, **21**, 191–220.

Thesis Abstract (Ph.D.)

On some problems in relativistic and non-relativistic hydro- and magnetohydrodynamics by M. S. Ganagi.
Research supervisor: A. V. Gopalakrishna.
Department: Applied Mathematics.

1. Introduction

The methods of singular surface theory and ray theory are very useful in the study of isotropic or anisotropic, homogeneous or inhomogeneous wave propagation in nonlinear continua[1,2]. In the presence of dissipative mechanisms where no real characteristics exist, these theories do not apply. But in some types of dissipative processes singular surfaces do exist[3]. When singular surfaces are disallowed, ideas of the wave-front theory provided by the above methods in combination with perturbation and asymptotic expansions provide a far-field description[4]. In fluid dynamics, steady, rotational, and universal motions constitute a very interesting class of flows. Methods of differential geometry are widely used in such a study[5].

2. Present study

By the use of the above methods problems studied in the present work are propagation of discontinuities in relativistic, inviscid, compressible fluids in the presence of finite electrical and heat conductivities[6], of pressure shocks in relativistic, viscous, heat-conducting fluids[7], and of weak discontinuities in arbitrarily moving relativistic magnetohydrodynamic fluids[8]. Also, relativistic analogue of generalised one-dimensional Burgers' equations is derived. The study of all the above problems is confined to flat space-time. Dealing with steady, rotational, and universal motions, aligned and orthogonal flows in non-relativistic incompressible, viscous, infinitely electrically conducting fluids are studied.

3. Conclusions

In the study on discontinuities, speeds of propagation of a discontinuity surface and the growth equation for the strength of the wave are obtained. In the case of finite electrical conductivity, a weak discontinuity grows into a shock in a finite time. In finite heat conduction, where the heat-flux-4-vector is of class $\mathscr{C}^1$ throughout the medium, a weak discontinuity exists only if the pressure is proportional to total energy density, while in the case of class $\mathscr{C}$, a singular surface exists only in low-temperature, and not in ultrarelativistic, case. The effect of dissipation is to cause damping. In the study of pressure shocks it appears that a time-like singular hypersurface is also possible in the case when pressure equals total energy density whereas in perfect fluids the usual shocks with this equation of state are necessarily null surfaces. The effect of curvature of the wave front on the strength of a weak discontinuity (fast or slow wave) when the medium ahead is at rest and in constant state is clearly brought out in the study of propagation of discontinuities in relativistic mhd. The form of relativistic Burgers' equation is the same as that of the classical case, the relativistic effect occurring only in the constant coefficients lowering the values of these for the perfect gas law. An analogue of Taylor's steady-state solution for strict one-dimensional case is presented. In classical mhd, some of the universal motions obtained are, for *e.g.*, in aligned flow, circular helical motion with certain properties of the velocity magnitude and in orthogonal case, no orthogonal, non-rectilinear magnetic field with non-vanishing electric current density is possible if the magnetic field lies in the plane determined by principal and bi-normal lines to the streamlines without coinciding with either of these directions.

References

1. THOMAS, T. Y. — Extended compatibility conditions for the study of surfaces of discontinuity in continuum mechanics, *J. Math. Mech.*, 1957, **6**, 311–322.
2. NARIBOLI, G. A. — Wave propagation in anisotropic elasticity, *J. Math. Analysis Applic.*, 1966, **16**, 108–122.
3. NARIBOLI, G. A. AND SECREST, B. G. — Weak discontinuities in magneto-gas-dynamics in the presence of dissipative mechanisms, *Tensor* (New Series), 1967, **18**, 22–25.
4. SEDOV, A., GOPALAKRISHNA, A. V. AND NARIBOLI, G. A. — Three-dimensional Burgers's equations in gasdynamics, *J. Phys. Soc. Jap.*, 1971, **30**, 557–561.
5. MARRIS, A. W. — Steady non-rectilinear complex-lamellar universal motions of a Navier-Stokes fluid, *Arch. Rational Mech. Analysis*, 1971, **41**, 354–362.
6. GANAGI, M. S. AND GOPALAKRISHANA, A. V. — Weak discontinuities in relativistic magnetohydrodynamics in the presence of dissipative mechanisms, to appear in *Int. J. Engng Sci.*

7. GANAGI, M. S. AND GOPALAKRISHANA, A. V. Pressure shocks in relativistic viscous heat-conducting fluids, *Astrophys. Space Sci.*, 1987, **129**, 281–292.

8. GOPALAKRISHNA, A. V. AND GANAGI, M. S. Weak discontinuities in relativistic mhd, *Astrophys. Space Sci.*, 1986, **120**, 139–149.

Thesis Abstract (Ph.D.)

Numerical studies of unsteady, double diffusive mixed convective boundary-layer flows by Savita Mahajan.
Research supervisor: G. Nath.
Department: Applied Mathematics.

1. Introduction

For flows about solid bodies, Prandtl[1] expounded that the viscosity effects are restricted to a thin boundary layer in the neighbourhood of the body when the fluid viscosity is small. This theory of Prandtl opened a totally new vista for research in fluid mechanics and the last couple of decades have seen many new developments. Laminar heat transfer has been investigated from the stand point of either pure free convection or pure forced convection. When the temperature difference between the surface and the ambient fluid is large, density differences arise which in turn give rise to buoyancy forces. These forces would possibly affect the momentum and heat transfer rates and thus it may not be justifiable to neglect the buoyancy effect on forced convective heat transfer. Such flows termed mixed convective flows occur in a variety of technological and industrial applications. Recently, Raju *et al*[2] have studied such flows past vertical and horizontal surfaces. A simultaneous heat and mass transfer resulting from the combined buoyancy effects of thermal and mass diffusion occurs in many transport processes. Gebhart and Pera[3] have conducted an interesting study for such double diffusive flows but for natural convection only. In the field of aerodynamics, we come across many unsteady flows where the unsteadiness occurs due to time-dependent body motion or disturbances in the surrounding flow field. The latter occurs when the free-stream velocity or the surface mass transfer or the wall temperature or all vary arbitrarily with time.

2. Present analysis

From an extensive literature survey, it was observed that unsteady mixed convective flows with double diffusion have not been investigated in spite of their various technological applications. The present work presents a numerical study of unsteady, incompressible, laminar mixed convective boundary layer flows with double diffusion over various geometries. The unsteadiness is assumed to be due to the free-stream velocity varying arbitrarily with time. Accelerating, oscillating and decaying profiles for the free-stream velocity have been considered. The analysis is confined to mass-diffusion processes with low concentration levels and covers the diffusion of various gases and vapors into air and water. The effects of various parameters such as unsteadiness viscous dissipation buoyancy forces due to temperature and concentration and mass transfer on the skin friction, heat transfer and mass transfer coefficients as well as on the velocity temperature and concentration profiles have been studied in detail.

Finite difference schemes are fast and efficient numerical methods. They are ideal to solve boundary-layer equations which are a set of nonlinear parabolic partial differential equations. In this

work the first three problems are solved using an implicit finite difference scheme in conjuction with the quasilinearisation technique as developed by Inouye and Tate[4]. Quasilinearisation possesses monotonicity and quadratic convergence and hence is a very efficient method. The last problem has been solved using a finite difference scheme along with Newton's linearisation technique. To do this with an efficient and stable scheme, a block-tridiagonal factorization scheme[5] is employed.

3. Conclusions

Mixed convection with mass transfer in the case of flow along a thin, long, vertical cylinder, cone, yawed cylinder and rotating sphere is investigated. The coefficients of skin friction and heat and mass transfer increase with net buoyancy forces and with transverse curvature. As the net buoyancy forces assisting the forced convective flow increases the velocity profile exhibits an overshoot in the vicinity of the wall. This effect is observed to diminish with the passage of time since the effects of buoyancy are suppressed by the growing inertical forces.

References

1. PRANDTL, D. — *Uber flussigkertsbewegung bei seh Kleiner Reibung.* Verh III Int. Math. Kong. Heidelberg 1904, 484 [English Transl., *Motion of fluids with very little viscosity*, NACA TM-452, 1928].
2. RAJU, M. S., LIU, X. Q. AND LAW, C. K. — A formulation of combined forced and free convection past horizontal and vertical surfaces, *Int. J. Heat Mass Transfer*, 1984, **27**, 2215–2224.
3. GEBHART, B. AND PERA, L. — The nature of vertical natural convection flows resulting from the combined buoyancy effects of thermal and mass diffusion, *Int. J. Heat Mass Transfer*, 1971, **14**, 2025–2050.
4. INOUYE, K. AND TATE, A. — Finite-difference version of quasilinearisation applied to boundary-layer equations, *AIAA J.*, 1974, **12**, 558–560.
5. CEBECI, T. AND SMITH, A. M. O. — *Analysis of turbulent boundary layers*, 1974, Academic Press.
6. MERKIN, J. H. — Mixed convection from horizontal circular cylinder, *Int. J. Heat Mass Transfer*, 1977, **20**, 73–77.

Thesis Abstract (Ph.D.)

Numerical solution of some unsteady boundary-layer flows by H. G. Datar.
Research supervisors: G. Nath and K. M. Agashe.
Department: Applied Mathematics.

1. Introduction

Unsteady boundary-layer flows are important in many engineering problems. Helicopter rotor, cascades of blades of turbomachinery and ship propeller normally operate on an unsteady aerodynamic environment. The present work is devoted to obtain numerical solution on certain problems in unsteady boundary-layer flows. Four different types of problems are considered: (i) Unsteady incompressible boundary layer for longitudinal flow over a cylinder with an applied magnetic field, (ii) Unsteady flow of heat and mass transfer on a stretching sheet, (iii) Effect of massive blowing on the unsteady compressible three-dimensional stagnation point boundary layer in the

presence of magnetic field, and (iv) Unsteady flow over an infinite rotating disk with an applied magnetic field (the fluid is at rest).

2. Problem formulation

The partial differential equations governing the flow have been written for the above problems. Some assumptions are made for writing these equations. For example, in the case of the first problem it is assumed that free-stream velocity distribution and surface mass transfer vary arbitrarily with time. In the problem of stretching sheet it is assumed that surface speed varies arbitrarily with time. In the last problem, it is assumed that disk is rotating with a time-dependent angular velocity.

3. Methods of solution

Unsteady boundary-layer equations which are written for these problems are highly nonlinear. The method of finite differences can be applied to solve these equations. Implicit finite difference scheme based on the Crank-Nicholson formulae is used in the problem of unsteady flow over a cylinder. In the case of stretching sheet the equations are solved by finite difference scheme with quasilinearization. To solve self-similar equations in the third problem an implicit finite difference scheme with variable step size along with quasilinearization technique is used. The reason for using a variable step size is that it keeps the stability of the numerical scheme. For unsteady flow over an infinite rotating disk the equations are solved by using Newton's linearization technique along with the finite difference.

4. Results and discussion

The effects of various parameters on skin friction and heat transfer have been considered for the above problems. In the problem of flow over a cylinder, it is observed that skin friction and heat transfer results are found to be strongly dependent on the magnetic field and surface mass transfer.

In the case of unsteady flow over a stretching sheet[2,3], the results indicate that skin-friction and heat-transfer parameters increase with time. The effect of suction is to decrease the boundary-layer thickness and stabilise the boundary layer while injection increases boundary-layer thickness and decreases stability.

The effect of large injection and magnetic field on the velocity and total enthalpy profiles has been studied in the third problem. The results indicate that velocity profiles show overshoot as magnetic parameter increases. However, in the case of enthalpy profiles such a trend is not observed.

In the problem of flow over a rotating disk the results are found to be strongly affected by the magnetic field and mass transfer. Magnetic parameter increases skin-friction coefficient in tangential direction but reduces skin coefficient in the radical direction.

References

1. LIU, T. M. AND CHIU, H. H. Fast and stable numerical method for boundary-layer flow with massive blowing, *AIAA J.*, 1976, **14**, 114–116.

2. GUPTA, P. S. AND GUPTA, A. S. Heat and mass transfer on a stretching sheet with suction or blowing, *Can. J. Chem. Engng*, 1977, **55**, 744–746.

3. BANKS, W. H. H. Similarity solutions of the boundary-layer equations for a stretching wall, *J. Méc. Théor. Appl.* 1983, **2**, 375–392.

4. TAKHAR, H. S., SURMA DEVI, C. D. AND NATH, G. Unsteady laminar incompressible boundary layer flows over a rotating disk with an applied magnetic field, *Indian J. Technol.*, 1987, **25**, 155–159.

Thesis Abstract (Ph.D.)

Stability of incompressible stratified fluid flows by S. Parhi.
Research supervisor: G. Nath.
Department: Applied Mathematics.

1. Introduction

Hydrodynamic and hydromagnetic instability is one of the most attractive branches of fluid dynamics. During the last fifty years it has been extensively studied[1-3] and found application in meteorology, oceanography, astrophysical and geophysical problems like the study of fluid dynamics of earth's core and propagation of gravity waves in the atmosphere from the troposphere to ionosphere. It has also wide range of applications in acoustics, many industrial problems like producing plastic films and sheets of synthetic materials, spinning of fibres, glass blowing and even in nuclear weapons, nuclear safety, inertial confinement fusion, etc. Since gravity is omnipresent and fluid homogeneity is an exception rather than a rule, the subject dealt with in this work is relevant to most flows occurring in nature.

2. Object and general method of the present investigation

The prime object of the present investigation is to find criterion or mechanism for stability or instability. Mathematically, the problem consists of following subsequent career of a hydrodynamically or hydromagnetically possible disturbance which is superposed on basic steady flow. If the disturbance vanishes as $t \sim \infty$, the motion is stable; otherwise, it is unstable. To study the behaviour of disturbances one must follow the solution of a system of nonlinear partial differential equations, which, in general, is very difficult. Instead one assumes that the disturbances are small so that the equations governing the disturbance may be linearized, *i.e.*, the terms quadratic or higher in the disturbances and their derivatives may be neglected. Consequently, a characteristic value problem is obtained with phase velocity C of the disturbance as parameter. When the disturbance has a time factor as $\exp(C_i)$ and if all the characteristic values of C have negative real parts, the motion is stable with respect to infinitesimal disturbance. If some of the characteristic values of C have positive real parts the motion is said to be unstable.

3. Stability of viscous flow over a stretching sheet

The boundary-layer stability of the viscous incompressible flow over a deformable sheet when the sheet is stretched in its own plane with an outward velocity proportional to the distance from a point on it is studied here. The perturbations are periodic in z having exponential time and x-dependence (direction of stretching). The small spanwise periodic x-velocity perturbation provides a small periodic component of vertical vorticity. Using Galerkin technique it is found[4] that the linearized flow due to stretching sheet is stable when the non-dimensional perturbation factor a along the direction of stretching (x-axis) is small and the product of this factor with another

non-dimensional wave number K (also small), along z-axis, depending on a, is much less than 1. The critical wave number K_c of z-dependent wave number required just to attain instability, for fixed x-dependent perturbation factor a, has been obtained and *vice versa*. When a decreases the threshold wave number K_c also decreases. But when $a \to 0$, K_c becomes constant which agrees with the earlier results[5].

4. Rayleigh-Taylor instability of viscous three-layer flow

Here, the work of Chandrasekhar[1] in Rayleigh-Taylor instability for two-layer incompressible viscous fluids to three-layer fluids pursuing a medium range wavelength analysis is studied. The wave Reynolds number in the middle thin layer is assumed to be very small but positive. Using a good approximation of different functions involved a new sufficient criterion for this instability is obtained depending on density stratification, viscosity ratios, wave number of perturbation, thickness of the middle layer and surface tension. The earlier results[1] are also recovered.

5. Stability of magnetohydrodynamic stratified shear flows

Here the stability of a stratified shear flow of a perfectly conducting bounded fluid in the presence of a magnetic field aligned with the flow and buoyancy forces has been studied under Boussinesq approximation. By using different bounds for definite integrals a new upper bound has been obtained for the range of real and imaginary parts of the complex wave velocity for growing perturbations. The upper bound depends on minimum Richardson number, wave number, Alfven velocity and basic flow velocity. This generalises the earlier estimate[6] for inviscid stratified flows and extends it to hydromagnetic case. Høiland's[7] necessary criterion for instability of hydrodynamic stratified homogeneous shear flow is modified and its analog for nonhomogeneous magnetohydrodynamic cases is derived. Finally, the upper bound for the growth rate of KC_i and its variants, where K is the wave number and C_i, the imaginary part of complex wave velocity, is derived as the necessary condition of instability. All estimates remain valid even when the minimum Richardson number J_1, for some practical problems, exceeds 1/4 for growing perturbations.

6. Over-reflection in Hartmann flow

The over-reflection in Hartmann flow using finite-difference technique is studied here. It is observed that Hartmann flow sustains wave propagation in its centre region for waves whose phase speed is less than the maximum flow speed. It is found that viscous boundary layers around the critical level and at the wall replace the exponential regions and wave sinks required for over-reflection in the inviscid flow. The uniform magnetic field stabilizes the flow for small wave number disturbance along z-direction. Over-reflection is confined to a few ranges of phase speeds rather than one range[8] for which the two boundary layers are close together rather than widely separated. These ranges correspond exactly to those for which unstable eigen modes exist. Over-reflection is associated with a wave phase speed tilted opposite in direction to the shear.

7. Conclusions

The result of this investigation can be extended to nonlinear disturbances. Rayleigh-Taylor instability can be studied for more than three-layer flows. Over-reflection problem can be undertaken for different types of flows. The study of over-reflection is now at very early stage.

References

1. CHANDRASEKHAR, S. — *Hydrodynamic and hydromagnetic stability*, 1961, Oxford University Press.
2. JOSEPH, D. D. — *Stability of fluid motions*, Vols 1 and 2, 1976, Springer-Verlag.
3. YIH, C. S. — *Stratified flows*, 1989, Academic Press.
4. PARHI, S. AND NATH, G. — Stability of viscous flow over a stretching sheet, *Acta Technica CSAV*, 1989, **34**, 389–409.
5. BHATTACHARYYA, S. N. AND GUPTA, A. S. — On the stability of viscous flow over a stretching sheet, *Q. Appl. Math.*, 1985, **43**, 359–367.
6. MAKOV, YU. N. AND STEPANYANTS, YU. A. — Note on the paper of Kochar and Jain on Howards's semicircle theorem, *J. Fluid Mech.*, 1984, **140**, 1–10.
7. HØILAND, E. — On two-dimensional perturbation of laminar flow, *Geofys. Publ.* (OSlo), 1953, **18**, No. 9, 1–12.
8. LINDZEN, R. S. AND RAMBALDI, S. — A study of over-reflection in viscous Poiseuille flow, *J. Fluid Mech.*, 1986, **165**, 355–372.

Thesis Abstract (Ph.D.)

Numerical studies of compressible rotating laminar boundary-layer flows by Somnath Bhattacharyya.
Research supervisor: G. Nath.
Department: Applied Mathematics.

1. Introduction

The study of rotational flows has long been recognized as an important branch of fluid dynamics because of its wide range of applications both in nature and technology. The problem of interaction of rotating flow with a stationary surface has drawn the interest of meteorologists for many years in connection with the study of tornadoes and hurricanes. The first publication in this area came through Von Karman[1], who considered the problem of the flow induced by an infinite rotating disk where the fluid far from the disk is at rest. By using a similarity principle, he was able to reduce the full system of Navier-Stokes equations to a pair of nonlinear ordinary differential equations in the axial coordinate. Von Karman similarity principle still applies when the problem is generalized to include the case where the fluid far from the stationary disk is exhibiting a solid body rotation[2] and to consider flow between two infinite coaxial rotating disks[3]. The question of the validity of Von Karman's approach in a finite geometry is of major importance and has been considered for incompressible fluid recently by Brady and Durlofsky[4]. The vortex motion in which the free stream is considered to vary as the power of the distance from the axis of rotation, *i.e.*, $v_\infty \sim r^{-n}$, is termed as a generalized vortex motion. Velocity of the form is found to be the best fit in describing certain motion in vortex chamber and in theoretical study of some atmospheric vortex. The boundary-layer equations describing a steady generalized vortex motion over an infinite disk can be reduced to a set of nonlinear ordinary differential equations for the case of incompressible[5] and compressible[6] fluid. Both steady and unsteady generalized vortex boundary layers of a compressible, electrically conducting fluid over a infinite porous disk have been studied. Effect of mass transfer and magnetic field on the flow is also included.

The study of magnetohydrodynamic spin-up (or spin-down) has importance in explaining certain geophysical or cosmological phenomena. A systematic study of the time-dependent flow of a rotating fluid describing the transient flow of initial and final rigid rotation in a spin-up process was initiated by Greenspan and Howard[7]. A detailed investigation has been made on hydrodynamic and hydromagnetic spin-up or spin-down of an electrically conducting compressible fluid. Initially, the motion is considered to be due to the uniform rotation of the disk in an otherwise stationary fluid or due to rigid-body rotation of the fluid over a stationary disk. Several cases of transient motion due to finite impulse imparted either to the disk or to the fluid at infinity are considered.

The generalized vortex boundary layer of a compressible fluid over a stationary disk of finite radius is considered. Effect of Mach number, radial distance and disk temperature on the flow and heat transfer has been investigated.

2. Results and conclusions

The governing boundary-layer equations are reduced to ordinary or partial differential equations by applying similarity or semi-similarity transformations. Numerical computations are carried out through finite-difference scheme along with Newton's linearisation or quasilinearisation technique.

The radial and azimuthal velocity profiles in the absence of magnetic field or suction approach their asymptotic values in an oscillatory manner and the amplitude of oscillation increases as n increases. Solutions can be obtained for a certain range of n in $[-1, 1]$. Magnetic field initiates a radial inflow when the disk is hot but for the cold disk radial velocity is predominantly outward. Suction ensures a radial inflow for both the cases. In the presence of magnetic field heat transfer increases with n but decreases when the effect of suction is considered. Heat transfer increases with the increase in the magnetic field and suction. An algebraic decay has been noticed for the hot disk case in the presence of a magnetic field.

The approach to the new steady state in a spin-up (or spin-down) process is found to be monotonic when the initial flow is induced by a rotating disk. For all cases magnetic field reduces the spin-up (or spin-down) time. In a hot disk, spin-up takes slightly less time compared to the cold disk. In spin-up all the velocities and wall values increase with time at the early stage and at the new steady state but the reverse trend occurs in spin-down, when the motion over a rotating disk is considered.

Skin friction in radial and tangential directions increases (decreases) steadily with time for an accelerating (decelerating) free stream. Rise of disk temperature increases the magnitude of both the wall shear components but reduces the magnitude of heat transfer. In a decelerating free stream, solutions are not obtainable after certain time in cold disk case even in rigid-body rotation ($n = -1$).

The velocity profiles are monotonic near the edge of the disk but they start exhibiting oscillation as the centre is approached. Heat transfer at the wall decreases as we proceed towards the centre from the edge of the disk but increases with n. Solutions exist for a certain radial distance for the entire range of $[-1, 1]$ of n. Increase of Mach number gives rise to a large increment in radial skin-friction component and heat transfer near the edge of the disk. Radial mass flux and axial velocity at infinity become higher with the rise of disk temperature.

References

1. Von Karman, T. *ZAMM*, 1921, **1**, 233–252.
2. Bodewadt, U. T. *ZAMM*, 1940, **20**, 241–253.
3. Batchelor, G. K. *Q. J. Mech. Appl. Math.*, 1951, **4**, 29–41.

4. BRADY, J. F. AND DURLOFSKY, L. *J. Fluid Mech.*, 1987, **175**, 363–394.
5. KING, W. S. AND LEWELLEN, W. S. *Phys. Fluids*, 1964, 7, 1674–1680.
6. BHATTACHARYYA, S. AND NATH, G. *Int. J. Engng Sci.*, 1989, **27**, 1639–1650.
7. GREENSPAN, H. P. AND HOWARD, L. N. *J. Fluid Mech.*, 1963, **17**, 385–404.

Thesis Abstract (Ph.D.)

Two-dimensional NMR spectroscopy in liquids: Developments in techniques and applications to polypeptides by K. Chandrasekhar.
Research supervisor: Anil Kumar.
Department: Physics.

1. Introduction

Two-dimensional (2D) nuclear magnetic resonance (NMR) spectroscopy, first proposed by Jeener in 1971[1], has grown at a rapid pace and now occupies a premier position as an analytical technique for the structure determination of biological macromolecules in solution. A variety of 2D NMR techniques is available, the most often used ones being correlated spectroscopy (COSY) and nuclear Overhauser enhancement spectroscopy (NOESY)[2–5]. Solution conformations of a large number of peptides and proteins have been determined using 2D NMR spectroscopy[6].

2. Results and discussion

The work deals with the basic principles of 2D NMR spectroscopy, with developments in techniques and application of these and other techniques to the conformational studies of three-membrane channel-forming polypeptides.

In the conventional COSY, the crosspeak multiplets have antiphase intensity character. This leads to poor crosspeak intensities under conditions of limited digital resolution, a situation often encountered in biological systems due to their large chemical shift dispersion. The diagonal peak multiplets, on the other hand, have inphase configuration leading to higher diagonal peak intensities. The proposed pulse scheme SUPER COSY utilizes fixed delays incorporated in the evolution and detection periods. These delays provide additional precession periods for the crosspeak multiplet components and bring them into inphase configuration. At the same time the diagonal multiplets become antiphase. Thus, the crosspeaks will have higher intensities compared to the diagonal peaks. Experimental results on a decapeptide LHRH are described showing the advantages of the proposed pulse scheme over the conventional COSY. Other 2D-correlated spectroscopies SECSY and RELAY COSY also have the same antiphase character for the multiplets (relay peak in RELAY COSY). Modified pulse schemes incorporating delays have been described for these spectroscopies also. The delay used is a function of coupling constant (J), spin-spin relaxation (T_2) and digital resolution (Hz/pt). An optimization procedure is described which allows an optimum delay to be chosen for a given set of J, T_2 and Hz/pt.

The results of 2D NMR experiments carried out on a 20-residue antibiotic peptide alamethicin in dimethyl sulfoxide solution have been described. By the combined use of SUPER COSY, RELAY COSY and NOESY spectra, almost total assignments have been obtained. By a careful analysis of the

NOESY spectrum, where a large number of sequential NOEs of the type N_iH to $N_{i+1}H(d_{NN})$ have been found, it was concluded that alamethicin adopts a largely helical conformation in organic solvents. Supporting evidence for such a conformation comes from the observation of $C^{\beta}H$–$N_{i+1}H(d_{\beta N})$ type NOEs, extensive intramolecular hydrogen bonding and small vicinal coupling constants (< 6 Hz).

The solution conformation of tetraacetyl melittin (TAM), a 26-residue polypeptide derived by acetylation of the bee venom peptide melittin in dimethyl sulfoxide has been described. A combined SUPER COSY–NOESY diagram[7] has allowed a large number of resonance assignments to be made. It was found that TAM consists of two segments of extended conformation between residue 7 to 11 and 15 to 18 with the remaining portion of the molecule being largely unordered.

NOESY results on a 16-residue synthetic analog of Zervamicin IIA (ZA1–16) have been described in chloroform. Complete resonance assignments have been obtained. It was delineated from the observed NOEs that ZA1–16 is largely helical in chloroform. Eleven of the 13 amide protons have been found to be intramolecularly hydrogen bonded. This is consistent with a helical conformation. The observed vicinal coupling constants further support the conclusions. The results are also compared with crystal structure data.

References

1. JEENER, J. — *Ampere International Summer School*, Basko Polje, Yugoslavia, 1971.
2. AUE, W. P., BARTHOLDI, E. AND ERNST, R. R. — *J. Chem. Phys.*, 1976, **64**, 2229–2246.
3. ANIL KUMAR, ERNST, R. R. AND WÜTHRICH, K. — *Biochem. Biophys. Res. Commun.*, 1980, **95**, 1–6.
4. ERNST, R. R., BODENHAUSEN, G. AND WOKAUN, A. — *Principles of nuclear magnetic resonance in one and two dimensions*, 1987, Clarendon Press.
5. CHANDRAKUMAR, N. AND SUBRAMANIAN, S. — *Modern techniques in high resolution FT-NMR*, 1987, Springer-Verlag.
6. WÜTHRICH, K. — *NMR of proteins and nucleic acids*, 1986, Wiley-Interscience (and references therein).
7. WAGNER, G., ANIL KUMAR AND WÜTHRICH, K. — *Eur. J. Biochem.*, 1981, **114**, 375–384.

Thesis Abstract (Ph.D.)

Studies on some technologically important deep level traps in gallium arsenide and gallium aluminium arsenide by Yashowanta N. Mohapatra.
Research supervisor: Vikram Kumar.
Department: Physics.

1. Introduction

This work is devoted to studies on electrical and optical properties of mainly three well-known, and yet not so well understood, technologically important deep levels in gallium arsenide and gallium aluminium arsenide. They are chromium-related traps and EL2 in semi-insulating GaAs, and the donor-related DX centre in GaAlAs.

2. Characterization of Cr-doped semi-insulating GaAs

Optical transient current spectroscopy (OTCS), also known as photo-induced transient spectroscopy (PITS)[1], is a convenient method of characterizing deep levels in semi-insulating material. However, there have been interpretational problems in applying the method to chromium-doped semi-insulating GaAs. We report two peaks[2], one positive and the other negative, in OTCS spectra of this material in the temperature range 300–450 K. The positive peak is due to a trap at $E_c - 0.47$ eV. The negative peak is attributed to the chromium-related midgap acceptor level at $E_v + 0.88$ eV. The anomalous negative peak is explained in terms of involvement of both electrons and holes in current transients. The photoconductivity spectrum of this material shows evidence of two intra-centre transitions in addition to optical thresholds corresponding to the two traps observed in OTCS spectra.

3. Studies on semi-insulating GaAs containing EL2

The main midgap electron trap in GaAs, commonly referred to as EL2, has many unusual and interesting properties[3], including its ability to get converted to an optically induced metastable state at low temperatures. The rate of conversion from the metastable to the normal state is thermally activated. A new and reliable method of measuring this activation energy in semi-insulating GaAs containing EL2 is proposed in this work. The technique, best described as thermally stimulated photocurrent (TSPC) method[4], consists of monitoring the temperature at which a step in photocurrent occurs due to the process of conversion as a function of heating rates. The analysis is analogous to thermally stimulated capacitance (TSCAP) method. The activation energy and the attempt-to-convert frequency for the process of conversion from the metastable to the stable state obtained by this method are critically compared with earlier reports. Also, photocurrent in semi-insulating GaAs containing EL2 is found to have unusual temperature dependence when EL2 is in its normal state. It increases exponentially with decreasing temperature down to about 50 K, beyond which it decreases slowly. We show that both extrinsic and intrinsic photocurrent in this material is due to the presence of EL2, though five different traps have been detected by OTCS and thermally stimulated current (TSC) measurements. The exponential increase of photocurrent with decreasing temperature is attributed to the temperature dependence of hole capture cross-section (σ_p) of EL2 in its normal state and the activation energy of σ_p has been inferred.

4. DLTS analysis for high-deep trap concentration

Deep-level transient spectroscopy (DLTS)[5] as a method of characterizing traps in semiconducting materials is described. Standard DLTS analysis for the cases of low ratio of deep trap to shallow trap concentration has been demonstrated using the results on the well-known iron-related hole trap in GaAs. The detection of an electron trap in *n*-type GaAs grown by liquid-phase epitaxy is also reported, a surprising result since no electron traps are expected normally in epitaxial layers of GaAs grown from Ga-rich solution. Often DLTS is also used to study traps in samples in which the ratio of concentrations of deep-to-shallow traps is very high. We draw broad useful conclusions regarding DLTS analysis in such cases of high-trap concentration through detailed simulations.

5. Trapping characteristics of donor-related DX centres in GaAlAs

Experimental DLTS spectra of DX centres in MBE-grown, silicon-doped $Al_xGa_{1-x}As$ ($x = 0.36$), recorded for varying filling pulse widths, show several interesting features, which make standard analysis inapplicable[6]. The significant features in the spectra are: interdependence of the two peaks; nearly logarithmic growth of peak heights, shift in the peak temperature, and reduction in width of

the lower temperature peak with increasing filling time. A qualitative phenomenological model of kinetics of DX centres is proposed based on the leading clues that the above features provide. The model proposed has the following features. The DX centre is the dominant donor having two states when filled, of which one is a metastable state. The charged state of the defect has a distributed energy barrier of capture[7]. On capturing the electron the trap first goes to metastable state from which it can get converted to the stable ground state by an Auger-like transition in the presence of free electrons. Both the states can emit electrons to the conduction band but the activation energy of emission of the metastable state gets lowered in the presence of electric field. In view of the complexities of the kinetics, no attempt has been made to numerically fit the experimental data. Through detailed calculations the plausibility of qualitative arguments is demonstrated and alternative possibilities ruled out.

References

1. KREMER, R. E., ARIKAN, M. C., ABELE, J. C. AND BLAKEMORE, J. S. — *J. Appl. Phys.*, 1987, **62**, 2424–2431.
2. MOHAPATRA, Y. N., BALASUBRAMANIAM, N. AND VIKRAM KUMAR — *Bull. Mater. Sci.*, 1985, **7**, 57–61.
3. MARTIN, G. M. AND MAKRAM-EBEID, S. — In *Deep levels in semiconductors* (ed.) S. T. Pantelides, 1985, Gordon and Breach.
4. MOHAPATRA, Y. N. AND VIKRAM KUMAR — *J. Appl. Phys.*, 1988, **64**, 956–958.
5. LANG, D. V. — *J. Appl. Phys.*, 1974, **45**, 3023–3032.
6. SUBRAMANIAM, S., ARORA, B. M., MOHAPATRA, Y. N. AND KUMAR, V. — *Proc. 14th Int. Conf. Defects in Semiconductors*, Paris, 1986, (ed.) H. J. von Bardeleben, Transtech, Switzerland.
7. CASWELL, N. S., MOONEY, P. M., WRIGHT, S. L. AND SOLOMON, P. M. — *Appl. Phys. Lett.*, 1986, **48**, 1093–1095.

Thesis Abstract (Ph.D.)

Experimental and modelling studies of glass structure by K. V. Damodaran.
Research supervisor: K. J. Rao.
Department: Solid State and Structural Chemistry Unit.

1. Introduction

For successful elucidation of structure of glasses, experimental and modelling approaches have to be adopted, depending on the nature of the system of interest and on the particular structural aspect under investigation. Various experimental methods of investigation include scattering techniques, X-ray spectroscopy, EXAFS, electron spin resonance (ESR), nuclear magnetic resonance (NMR) and measurement of elastic properties using ultrasonic method. Modelling of structure of glasses using molecular dynamics (MD) and Monte Carlo (MC) has also been widely adopted. Elastic properties of glasses are very sensitive to their detailed structure. The factors that determine the elastic moduli depend on the chemical nature of the glass system also. Thus, in covalent network glasses it is

convenient to relate these features through the size and concentration of various atomic rings. In purely ionic systems, however, the determining factor is the packing of ions or structural groups. Elastic properties of phosphomolybdate and phosphotungstate glasses (MoO_3–P_2O_5 and WO_3–P_2O_5) have been performed to investigate their structure. These are network glasses, built up of octahedral $[MO_{6/2}]$ (M = Mo, W) and tetrahedral $[PO_{3/2}]$ units. In these glasses a variety of structural changes can be brought about by the addition of alkali oxides or PbO. Variation of elastic properties with compositions have been utilized to draw valuable conclusions regarding the glass structure. The pair distribution functions obtained in molecular dynamics and Monte Carlo simulations may be effectively used to obtain the local structures present in the system. The technique can be used to obtain information on dynamical properties also. MD simulation has been adopted to investigate the structure of three glass systems—lead oxyhalides, silver borates and lead silicate.

2. Experimental

Glasses have been prepared from analar grade MoO_3, WO_3, $(NH_4)_2HPO_4$, alkali oxides and Pb_3O_4. Densities and glass transition temperatures have been measured. Ultrasonic velocities at 10 MHz have been measured using pulse superposition method. Molecular dynamics simulations have been performed using the Born-Mayer-Huggins pair potentials on MICROVAX-II computer.

3. Results and discussion

Effect of modification by alkali oxides on the elastic properties of phosphomolybdate and phosphotungstate glasses and their structural consequences have been investigated from their elastic properties[1,2]. The local structural environment of alkali ions rearrange in such a way that alkali ions acquire preferred oxygen coordinations, which in turn depend on the size and charge on the alkali ion. The resultant structural rearrangements in the glass network give rise to different atomic rings involving M–O–M, M–O–P and P–O–P linkages. Consequently, the average ring size decreases in Li_2O-containing glasses, while in Na_2O- and K_2O-containing glasses, it increases progressively. Elastic properties of these glasses show dependence on the concentration of alkali oxides, suggestive of this structural approach. The composition dependence of elastic properties of these glasses has been interpreted in terms of these atomic rings, their sizes and their disposition. Highly modified glasses exhibit bulk modulus volume relationships close to that of typical ionic systems. The nonlinear variation of physical properties in a glass containing more than one alkali oxide when their relative concentration changes has been known for a long time and is referred to as mixed alkali effect. Elastic properties of phosphomolybdate glasses containing (Na_2O, K_2O) and (Li_2O, K_2O)-mixed alkali couples have been found to exhibit pronounced nonlinearities in their composition dependence[3]. This appears to be due to the presence of two different kinds of modifier cations which gives rise to ring reformations in which minimum (optimum) number of smaller rings in the parent phosphomolybdate glass network are broken. The composition dependence of elastic moduli, Poisson's ratio and Debye temperature are in conformity with the strutural model involving two different atomic rings conserving the number of smaller rings in the structure.

Addition of PbO produces interesting structural changes in the phosphomolybdate and phosphotungstate system[2-4]. In glasses, certain cations have been found to act both as network former and network modifiers. Physical properties like density, molar volume and elastic moduli exhibit discontinuities in their composition dependence when the structural role of the cation in question changes. Elastic properties of PbO–MO_3–P_2O_5 (M = Mo, W) glasses have been investigated to understand the structural role of lead. The composition dependence of elastic properties suggests that at low concentrations Pb takes network-forming positions. The process is facilitated by the conversion of $[PO_{3/2}]$ units into $[PO_{4/2}]$ units, by which oxygen sharing and charge balance

requirements are satisfied. The results have confirmed some key aspects of the structural model proposed earlier for these glasses based on other physical property studies.

$PbO-PbF_2$ is an interesting vitreous system from the point of both structure and bonding. Earlier investigations of this system employed a number of experimental techniques such as X-ray and neutron diffraction, EXAFS, XANES and probe-ion spectroscopy. A structural model had been proposed according to which structural motifs $[PbO_2F_4]$ and $[OPb_4]$ were present throughout the glass-forming region. The presence of $[OPb_4]$ units is crucial for glass formation, since it forms the basis for continuous O–Pb–O chains. From the point of view of the nature of bonding, $PbO-PbF_2$ glass is an exemplary system in which the bonding varies continuously from covalent to ionic as composition varies from PbO-rich to PbF_2-rich regime. This is because PbO is a typical covalent system and PbF_2 is predominantly ionic. A molecular dynamics simulation of this system has been carried out to investigate the correspondence between the simulated structure and the proposed model[5]. The simulated structure supports many of the experimental findings, especially the presence of $[OPb_4]$ units. In the simulated structure, oxygen and fluorine coordinations of Pb vary. A detailed discussion of the pair distribution functions (PDFs), diffusion and velocity autocorrelation functions is presented. The radial distribution function obtained from the PDFs by the pair function method is compared with the one obtained in earlier X-ray diffraction studies.

A molecular dynamics study of silver borate glasses has been performed[6] mainly to understand the local environment of silver atoms. The observed pair distribution functions suggest a fairly random distribution of silver. However, the results show some disagreement with EXAFS results of this system available in literature, with regard to oxygen coordination number. This has been attributed to the non-directional nature of the pair potential used in molecular dynamics simulations.

A molecular dynamics simulation of $PbO-SiO_2$ glass and melt structures has been performed[7] to investigate the local structure in this system. In $PbO-SiO_2$ system, lead, at low concentrations, acts as a network modifier, but in high-PbO glasses takes network-forming positions also. The observed Pb–Pb correlation shows good agreement with X-ray diffraction results. Si–Si PDFs show interesting differences between vitreous silica and $PbO-SiO_2$ which may be due to folding of Si–O–Si chains. The observed Pb–O PDFs in MD studies shows an oxygen coordination number of 5 for lead. However, X-ray diffraction studies available in this system suggest somewhat lower oxygen coordination number for lead which forms PbO_4 pyramidal units. The latter view is based purely on crystallographic considerations and does not appear to take into account the fraction of lead modifying the silica network. The discrepancy between X-ray diffraction and simulation studies could also be partly as a result of the spherical nature of the pair potential as mentioned in the case of $Ag_2O-B_2O_3$ glasses.

References

1. DAMODARAN, K. V. AND RAO, K. J. — *J. Am. Ceram. Soc.*, 1989, **72**, 533–539.
2. DAMODARAN, K. V. AND RAO, K. J. — *J. Mater. Sci.*, 1989, **24**, 2380–2386.
3. DAMODARAN, K. V. AND RAO, K. J. — *Phys. Chem. Glasses*, 1989, **30**, 130–134.
4. DAMODARAN, K. V., SELVARAJ, U. AND RAO, K. J. — *Mater. Res. Bull.*, 1988, **23**, 1151–1158.
5. DAMODARAN, K. V. AND RAO, K. J. — *Chem. Phys. Lett.*, 1988, **148**, 57–61.
6. RAO, B. G., DAMODARAN, K. V. AND RAO, K. J. — *J. Non-crystalline Solids* (communicated).
7. DAMODARAN, K. V., RAO, B. G. AND RAO, K. J. — *Phys. Chem. Glasses*, 1990, **31**, 212–216.

Thesis Abstract (Ph.D.)

Dharwar stratigraphy and gold mineralisation in Kolar supracrustal belt, Karnataka Craton, India by G. S. Anil.
Research supervisor: G. V. Anantha Iyer.
Department: Inorganic and Physical Chemistry.

1. Introduction

The Archean Peninsular Gneissic Complex (PGC) in Karnataka Craton, of tonalite-trondhjemite-granodiorite composition, unconformably underlies the late-Archean, early-Proterozoic mafic platformal and geosynclinal succession of the Dharwar supracrustals. The analysis and synthesis of geological and geochronological data[1] have helped establish the chronostratigraphic relationships between the chief crustal components of the Western Block (Table I).

In the eastern part, the PGC yields an Rb–Sr age close to 3000 Ma. and the intrusive granites date at around 2600 Ma. The cordierite gneiss enclaves, dated by Rb–Sr method at 3010 Ma[2] are correlated with the Sargur Group. The Kolar supracrustal succession yields a Pb–Pb age of 2700 Ma. and is considered a facies variation of the Bababudan Group[3]. The metavolcanic succession of Hutti dates at about 2350 Ma. which is close to that of the Chitradurga Group.

The study of the evolutionary history of the Dharwar belts suggests a number of broad controls on the distribution pattern of the gold deposits.

The Sargur Group is almost barren of gold probably because of early silicification, absence of suitable fluid components and unfavourable metamorphic style. The mafic sequences of the Bababudan

Table I
Chronostratigraphy of the Western Block

Components		Lithounits	Age
Dharwar *Supergroup*	Chitradurga Group	Deep-water, shelf and geosynclinal facies	2345 Ma.
	Bababudan Group	Shallow-water mafic platformal facies	2620 Ma.
	----------UNCONFORMITY----------		
Peninsular Gneiss	Tonalite-trondhjemite-granodiorite components		3000–3200 Ma.
Sargur Group	Ultramafic-mafic volcanics and minor anorthosites linked to orthoquartzites-metapelites-amphibolites-banded iron stones		3095–3180 Ma.
Gorur-Hassan Gneiss	Tonalite-trondhjemite-granodiorite components		3300 Ma.

Group are subaerial and correspond to sulphide- and gold-depleted source rocks and do not contain any significant gold[4]. The low-grade ore in the deposits of the western Dharwar belts can be attributed to the dominance of sediments and low-grade of metamorphism. The volcanic dominant belts of the eastern Dharwar are shown to have the right combination of rock types and metamorphic history to offer excellent conditions for gold mineralisation.

2. Kolar Gold Fields

Based on the detailed study of the underground working of the Kolar Gold Fields, a viable genetic model for gold mineralisation is proposed (Table II).

Detailed petrographic studies of the metavolcanic succession reveal that they are fine- to coarse-grained. The pillow, variolitic and amygdular structures preserved in the metabasalts suggest a predominantly subaqueous environment of eruption. Additional evidences for this are the quench plagioclase textures and glomeroporphyritic basalts which have been identified. Mineralogical studies show that the basalts have been metamorphosed to amphibolite grade.

Geochemical investigations suggest that the basalts are Fe-rich tholeiites which have undergone some degree of fractional crystallisation[5]. Chondrite-normalised REE patterns reveal that the central and the western sequences were generated from an LREE-depleted mantle source similar to that of MORB while the eastern succession appears to have been generated from LREE-enriched source. The high-Mg basalts, manifest as fibrous amphibolites, do not seem to be genetically related.

3. Controls of gold mineralization

Three types of bodies have been recognised in the belt. They are:

(i) Sulphide facies BIF-type: weak mineralisation,
(ii) Oriental type: sulphide-rich gold-quartz veins, and
(iii) Champion type: sulphide-poor gold-quartz veins.

All three types display strict stratigraphic control in that their occurrence is restricted to the contacts of different basaltic flows[6]. Another feature which they share is the parallel layering of quartz,

Table II
Lithostratigraphy of Kolar supracrustal belt

Western succession	Eastern succession
Dolerite dykes and pegmatites	Dolerite dykes and pegmatites.
Patna granite	Bisanattam granite
Metabasalts with sulphide-rich gold-quartz lodes	Metabasalts with sulphide-poor gold-quartz lodes
	Champion Gneiss Formation with polymict conglomerate
Yerrakonda Formation: Meta-basaltic succession with sulphide facies BIF	Yerrakonda Formation
Archean basement gneiss and Sakarsanite series	Archean basement gneiss and Sakarsanite series

sulphides, carbonates, silicates and oxides. The least radiogenic and the highly radiogenic Pb isotopes from all three types of lodes yield a common model age of 2650 Ma. The similarities of the lodes offer unequivocal evidence for their common origin as syngenetic stratiform deposits.

Using fluid inclusions, sulphide thermometry, silicate chemistry and stable isotope chemistry it has been shown that gold was transported and deposited by slightly alkaline hydrothermal solutions at a temperature of around 350 °C. Gold was carried in solution in the form of thio-complexes; the pH, sulphur fugacity and oxygen fugacity were calculated to be around 6, 10^{-11} and 10^{-31}, respectively.

4. Conclusions

The genetic model proposed for gold mineralisation in the Kolar Gold Fields, which takes into account all the similarities and differences in the mode of mineralisation, can be summed up thus:

1) Submarine Fe-rich tholeiitic volcanism took place around 2700 Ma. with resulting basalt-seawater reaction giving rise to the Oriental- and BIF-type stratiform and stratabound chemical sediments.
2) The resulting hydrothermal solutions, typically rich in CO_2 and H_2S, leached gold and sulphur from the host rock and transported them as thio-complexes at a temperature of around 350 °C.
3) Deposition of gold took place due to hydraulic fracturing causing a sudden drop in pressure and resulting in the sulphidation of the wall rock, change in pH and a drop in temperature accompanied by a loss of volatiles. This happened around 2650 Ma.
4) Later deformation and metamorphism, between 2300 and 1930 Ma., resulted in remobilisation and concentration of gold.

References

1. Swami Nath, J. and Ramakrishnan, M. — Early precambrian supracrustals of Southern India, *Mem. Geol. Surv. India*, 1981; **112**, 1–350.
2. Jayaram, S., Venkatasubramanian, V. S. and Radhakrishna, B. P. — Rb–Sr ages of cordierite gneisses of southern Karnataka, *J. Geol. Soc. India*, 1976, **17**, 557–561.
3. Hanson, G. N., Krogstad, E. J. and Rajamani, V. — Tectonic setting of the Kolar schist belt, Karnataka, India, extended abstract, *J. Geol. Soc. India*, 1988, **31**, 40–42.
4. Keays, R. R. — Archean gold deposits and their source rocks: the upper mantle connection, In *Gold' 82*, Foster, R. P. (ed.), 1984, pp 17–51, A. A. Balkema.
5. Anantha Iyer, G. V. and Vasudev, V. N. — Geochemistry of the Archaean metavolcanic rocks of Kolar and Hutti gold fields, Karnataka, India, *J. Geol. Soc. India*, 1979, **20**, 419–432.
6. Narayanaswami, S., Ziauddin, M. and Ramachandra, A. V. — Structural control and localisation of gold bearing lodes, Kolar Gold Fields, India, *Econ. Geol.*, 1960, **55**, 1429–1459.

Thesis Abstract (Ph.D.)

Chlorite-clay minerals from Chitradurga and Holenarasipur belts, Karnataka Craton, India: Progressive changes through diagenesis and metamorphism and application to copper mineralisation by B. V. Mohan.

Research supervisors: G. V. Anantha Iyer and A. G. Menon.
Department: Inorganic and Physical Chemistry.

1. Introduction

The Precambrian granite-greenstone terrain of Karnataka in the southern Indian Shield comprises a spectrum of erosional levels within the Archean crust. The Chitradurga Group (2345 Ma)[1] is well preserved in the central part of the Chitradurga belt while the platformal sequence of the Bababudan Group (2620 Ma)[2] and the Sargur Group (3095 Ma)[3] are exposed in the Holenarasipur belt. These units are coaxially folded due to superposed deformational events[4].

Ubiquitous in the lithostratigraphic units of Chitradurga, Bababudan and Sargur groups are the complex and the least studied chlorite minerals while in the geosynclinal sequence of the Chitradurga Group, clay minerals are preponderant. Detailed studies on the structure and chemistry of the chlorites and characterisation of the clay minerals have been carried out to provide information on the diagenetic-metamorphic history of the craton and the physico-chemical conditions of copper mineralisation in the Chitradurga belt.

Techniques used to study the chlorite-clay minerals are X-ray diffraction, chemical analysis, infrared spectroscopy, differential thermal analysis and scanning electron microscopy. The changes observed in these environmentally sensitive group of sheet silicates through diagenesis and metamorphism have been documented and different geological environments have been identified.

2. Diagenesis

A scheme for the diagenetic clay-chlorite mineral transformation in the Hiriyur, Ingaldhal and Vanivilas Formations of the Chitradurga Group is provided in Fig. 1. The clay minerals identified in the Hiriyur Formation are smectite, illite, corrensite, kaolinite and regularly interstratified chlorite-illite. The clay mineral transformation from smectite to corrensite at the expense of kaolinite suggests low-grade diagenesis conditions under shallow burial. The abundant Ib chlorite polytypes and their mixtures in the Ingaldhal Formation suggest their formation from smectite through an intermediate corrensite indicate high-grade diagenesis under deep burial conditions. The presence of IIb chlorites in the Vanivilas Formation marks the beginning of low-grade metamorphism. Further, textural evidence corresponding to different stages in diagenesis comparable to those described by Frey[5] lends support to the clay-chlorite transformation presented.

3. Metamorphism

Unlike the chlorites of the Chitradurga Group, the chlorites from the Bababudan and Sargur groups are IIb polytypes and indicate their metamorphic origin. The study of the mineral reactions responsible for the chlorite-bearing assemblages preserved in the Bababudan group suggest that they were formed under greenschist facies conditions within the stability field of chloritoid (350 to 550 °C at 5 kbar). Those from the Sargur Group were formed under amphibolite facies within the stability field of staurolite (550 to 700 °C between 5 and 7 kbars). Compositionally, these IIb polytypes are Mg-rich in comparison with Ib chlorites of the Chitradurga Group.

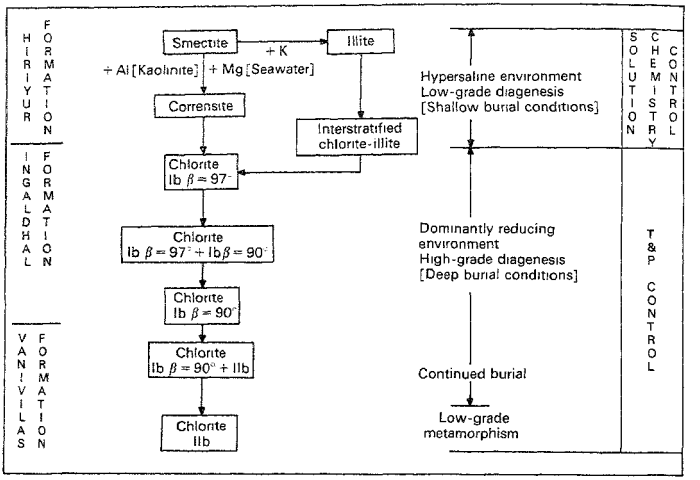

FIG. 1.

4. Physico-chemical conditions of copper mineralisation

The physico-chemical conditions of the copper deposits in the Ingaldhal Formation have been evaluated based on the structural and chemical characteristics of the chlorites from the wall-rock alteration zone, sulphide mineralogy, stable isotope geochemistry and thermodynamics of the chlorite-hydrothermal fluid reaction. Fluid parameters have been estimated using reactions involving chlorites and fluid components and assuming an ideal mixing model for chlorite end members[6]. A new approach involving chlorite polytypism as a geothermometer has been used to fix the temperature of the mineralising solution. The estimated solution parameters are *T*: 200 °C, P: 1 kbar, pH: 5.0, $f(O_2)$: $10^{-41.95}$ to $10^{-43.30}$ and $f(S_2)$: $10^{-12.50}$ to $10^{-14.10}$. The Ib chlorites from the wall rocks and the associated sedimentary structures suggest the diagenetic conditions of their formation and it is probable that mineralisation took place while the volcaniclastic sediments were undergoing diagenesis. The chemical variation observed in the wall rocks has been explained as a function of oxygen and sulphur fugacities, the Fe-rich chlorites forming under low $f(O_2)$ and $f(S_2)$ conditions.

References

1. CRAWFORD, A. R. *J. Geol. Soc. India*, 1985, **10**, 117–166.

2. DRURY, S. A., HARRIS, N. B. W., HOLT, R. W., REEVES-SMITH, G. J. AND WIGHTMAN, R. T. *J. Geol.*, 1984, **92**, 3–20.

3. KUTTY, T. R. N., ANANTHA IYER, G. V., RAMAKRISHNAN, M. AND VERMA, S. P. — *Lithos*, 1984, **17**, 317–328.

4. RAMAKRISHNAN, M. AND VISWANATHA, M. N. — *Mem. Geol. Soc. India*, 1981, **112**, 115–141.

5. FREY, M. — *Low temperature metamorphism*, Frey, M. (ed.), 1987, pp 9–58, Blackie.

6. WALSHE, J. L. — *Econ. Geol.*, 1986, **81**, 681–703.

Thesis Abstract (Ph.D.)

Methyl methacrylate, styrene and vinylnaphthalenes polymeric peroxides: Syntheses and physico-chemical behaviour by T. Mukundan.
Research supervisor: K. Kishore.
Department: Inorganic and Physical Chemistry.

1. Introduction

Polymeric peroxides[1] are an important class of compounds and are the polymeric counterparts of the low-molecular weight peroxides, commonly encountered in polymer chemistry as initiators, cross-linking agents, etc. The formation and degradation of polyperoxides have been studied mainly from the point of view of their usefulness in explaining the inhibitory role of oxygen in vinyl polymerization[2]. The physical and chemical properties of this class of polymers thus remain largely unexplored[3]. It was only recently[4] that studies from our laboratory identified in-chain peroxy intermediates in propellant combustion, formed by the union of monomer formed during the combustion of the binder with oxygen generated from oxidizers. With this background, it was thought desirable to look into the fuel behavior of heat-in-chain polyperoxides, in preference to that of the conventional binders. One of the important aspects of the present investigation deals with this, with poly(styrene peroxide), PSP, as the chosen substrate. Syntheses of new polymeric peroxides have also been accomplished keeping in view their potential fuel characteristics. The development of a new initiating system based on PSP for the room temperature vinyl polymerization also explored successfully during the present study is an attempt to look into the chemical properties of this class.

2. Important results

2.1. *Syntheses and characterization of new polymeric peroxides*[5,6]

Three new polymeric peroxides based on vinyl and substituted vinylnaphthalenes, *viz.*, poly (1,α-methylvinylnaphthalene peroxide) (PMVNP 1), poly (2,α-methylvinylnaphthalene peroxide) (PMVNP 2) and poly (2-vinylnaphthalene peroxide) (PVNP 2) were synthesized. They were characterized by ir, ^{1}H and ^{13}C nmr spectroscopy. Poly (methyl methacrylate peroxide) (PMMAP), whose synthesis was known in literature, was given a spectroscopic conformation of its structure using ir, Raman, ^{1}H and ^{13}C NMR spectroscopy.

2.2. *Thermal degradation*[5-7]

The thermal degradation of all the above-mentioned polyperoxides was studied using thermal analysis and pyrolysis gas chromatography (PGC) techniques. The heats of degradation of the various polymers measured by differential scanning calorimeter (DSC) were: PMMAP, -44 ± 2 kcal mol^{-1}; PVNP 2, -49 ± 1 kcal mol^{-1}, PMVNP 1, -53 ± 2 kcal mol^{-1} and PMVNP 2, -53 ± 2.5 kcal mol^{-1}. The products of thermal degradation (analyzed by PGC) were formaldehyde and corresponding aldehyde or ketones, accounting for 95% of the total products in all cases.

2.3. *Thermochemical calculation*[5,7]

The experimental data on the thermal degradation of PMMAP have been corroborated using thermochemical calculations. Thermochemical data available in literature and computed by group additivity method were used in the calculations. The experimental and calculated values of heats of degradation were closely matching.

The activation energy for the degradation process was found to correspond to the scission of the O–O bond. Based on these results a radical chain scission mechanism has been proposed for the degradation of PMMAP and is applicable in the case of other polymers as well.

2.4. *Phenomena of auto-pyrolysis and auto-combustion in polymers*[8]

For the first time in polymers, poly(styrene peroxide), PSP, was shown to exhibit auto-pyrolysis and auto-combustion. The highly exothermic heat of degradation of PSP enables it, once initiated, to burn uninterruptedly with a rate comparable to that of solid propellants. The combustion was proved to be directly controlled by the degradation. Additivies behaved in identical fashion both in degradation and combustion of PSP. For instance, while *p*-toluidine accelerated both, nitrobenzene decelerated them. PGC studies showed that no new products were formed in the degradation of PSP in the presence of additives.

2.5. *A novel class of fuel based on polyperoxides*

PSP with an oxidizer, ammonium perchlorate (AP), loading of 30–35% by weight, exhibited self-supported combustion. This extent of oxidizer loading is far less, compared to the generally required minimum (60–70% by weight) of oxidizer content in conventional rocket propellants. An unexpected maximum in the linear burning rate was observed in the PSP-AP slurry, with 5% AP content. DSC studies verified this observation and showed a sensitization of 10° in the peak temperature of PSP degradation, in a slurry of the same composition.

2.6. *Application of the chemical reactivity of PSP*[9]

PSP in the presence of diethylamine (DEA) was found to initiate radical polymerization of acrylamide, methyl methacrylate and styrene at room temperature. It was found that this system was more efficient than benzoyl peroxide-DEA system at room temperature. The initiation of PSP-DEA system was proved to be of a radical nature.

References

1. MUKUNDAN, T. AND KISHORE, K. Synthesis, characterization and reactivity of polymeric peroxides, *Prog. Polym. Sci.*, 1990, **15**, 475–505.

2.	BHANU, V. A. AND KISHORE, K.	Role of oxygen in polymerization reactions, *Chem. Rev.*, 1991 (in press).
3.	MUKUNDAN, T. AND KISHORE, K.	Recent advances in exploring the physico-chemical properties of polyperoxide, *Curr. Sci.*, 1991 (in press).
4.	KISHORE, K., PAI VERNEKAR, V. R. AND GAYATHRI, V.	*Fuel*, 1981, **60**, 164–168.
5.	MUKUNDAN, T. AND KISHORE, K.	*Macromolecules*, 1987, **20**, 2382–2385.
6.	MUKUNDAN, T. AND KISHORE, K.	*Macromolecules*, 1989, **22**, 4430–4433.
7.	KISHORE, K. AND RAVINDRAN, K.	*Macromolecules*, 1982, **15**, 1638–1639.
8.	KISHORE, K. AND MUKUNDAN, T.	*Nature*, 1986, **324**, 130–131.
9.	MUKUNDAN, T., BHANU, V. A. AND KISHORE, K.	*J. Chem. Soc., Chem. Commun.*, 1989, **12**, 780–781.

Thesis Abstract (Ph.D.)

Role of oxygen and *bis*(N-arylsalicylaldimino) cobalt(II) complexes in radical polymerization

by V. A. Bhanu.
Research supervisor: K. Kishore.
Department: Inorganic and Physical Chemistry.

1. Introduction

Oxygen is known to either initiate or inhibit free radical vinyl polymerization[1]. Although peroxide formation reaction is considered to explain the retarding action of oxygen, its thermal instability renders the retarding action of oxygen temperature dependent. Hence, it is desirable to manifest this role of oxygen in a different manner.

Tetrahedral Co(II) complexes derived from Schiff bases of salicylaldimines show unusual flexibility of the ligand core to accommodate extra ligands[2]. It is interesting, therefore, to study the effect of these complex additives in the kinetics of radical polymerization.

2. Important results

1. The rapid and simple method of differential scanning calorimetry (DSC) has been used to demonstrate the retarding action of oxygen during the melt polymerization of acrylamide, in terms of the shift in peak temperature of polymerization exotherm to a higher value in the presence of oxygen[3].

2. Redox couple based on $Co^{+2}/NaBH_4$ (where Co^{+2} indicates the tetrahedral Co complexes derived from salicylaldimine ligands) is found to initiate radical polymerization of styrene at room temperature. More interestingly, if the above reaction is carried out in air, styrene oxidizes *via* a peroxide intermediate to 1-phenyl ethanol. This indicates that in the presence of oxygen the above polymerizable system yields a thermally stable, non-peroxidic end product. Hence, the above experiment also proves that it is possible to render the inhibitory action of oxygen in radical polymerization temperature independent[4].

3. The effect of cobalt complexes A and B as additives on the AIBN-initiated bulk polymerization of styrene and MMA has been studied by dilatometry. A higher induction period (of the order of

several minutes) has been observed in the MMA polymerization as compared to that in the styrene polymerization. This is explained on the basis of the preference of propagating radicals of MMA to propagating radicals of styrene in their reaction with the cobalt complexes. The rate of polymerization should decrease in the presence of additives since the concentration of radicals decreases in their presence. Although this expectation turns out to be true for styrene polymerization, an acceleration is nevertheless observed in the rate of MMA polymerization. Furthermore, the order of reaction with respect to the monomer is higher than unity in the presence of A and B, which suggests a deviation from the normal radical polymerization. Normally such a higher order with respect to the monomer in the radical polymerization implies participation of the monomer in the initiation step. The increase in the rate of polymerization of MMA in the presence of A or B seems therefore to be due to increase in the rate of initiation in the process of polymerization. A mechanism which accounts for the above two anomalies and the fact that the original complex (A or B) is regenerated at the end of the reaction has been proposed.

4. DSC study of the melt polymerization of acrylamide in the presence of complexes A–D has been carried out. While thermal polymerization is strongly inhibited by these additives, only an induction period is imparted to the AIBN-initiated acrylamide polymerization. The radical quenching reaction of the complexes A–D is found to be responsible for these observations.

5. The Schiff base ligands employed for the preparation of the cobalt complexes have been found to exhibit an unusual conformational sensitivity[5] on the basis of the correlations carried out using their ^{13}C NMR data[5]. The ligands derived from salicylaldehyde and anilines have twisted conformations, while those derived from 5-methyl-salicylaldehyde and anilines have planar conformation.

Some novel observations on the comparative study of the thermal and thermo-oxidative degradation of a few vinyl polymers have been explained[6].

References

1. BHANU, V. A. AND KISHORE, K. — Role of oxygen in polymerization reactions, *Chem. Rev.*, 1991 (in press).
2. BHANU, V. A. AND KISHORE, K. — *J. Polym. Sci. Chem. Ed.*, 1990, **28**, 3617–3624.
3. KISHORE, K. AND BHANU, V. A. — *J. Polym. Sci. Chem. Ed.*, 1986, **24**, 53–55.
4. BHANU, V. A. AND KISHORE, K. — *Macromolecules*, 1989, **22**, 3492–3494.
5. KISHORE, K., SATHYANARAYANA, D. N. AND BHANU, V. A. — *Magn. Resonance Chem.*, 1987, **25**, 471–473.
6. KISHORE, K. AND BHANU, V. A. — *J. Polym. Sci. Lett. Edn*, 1985, **23**, 567–571.

Thesis Abstract (M.Sc. (Engng))

Design, development and performance evaluation of a digital quartz crystal monitor for thin film deposition by L. Shivalingappa.

Research supervisors: S. Mohan and M. P. Srinivasan.
Department: Instrumentation and Services Unit.

1. Introduction

Thickness is one of the most important parameters of the thin films since it largely determines the properties of a film. On the other hand, almost all the properties and structure of thin films depend on the thickness.

Because of the importance of thickness measurement of thin films, it has been decided to design and develop a stable quartz crystal monitor for computing the rate of evaporation and the thickness of the films during deposition. The design, fabrication and testing of the monitor and its performance in measuring thickness of different materials evaporated in a 20″-evaporation system are presented in this work.

Quartz crystal monitors based on the principle of change in the resonant frequency of a quartz crystal due to mass loading have been used for thickness monitoring[1]. This has been done by improving the electronic circuits by selecting crystals with very low variation in frequency with temperature[2] and by using the same crystal for monitor and reference oscillators[3,4]. A number of additional features like provision to measure the rate and thickness of the film directly in angstroms by setting the density of the evaporating material and, termination of the deposition at required thickness have also been incorporated in the monitor.

2. Circuit description

The electronic subsystems of the monitor (Fig. 1) are monitor and reference crystal oscillators, frequency mixer, sampling interval generator, gating circuit, rate counter, rate display unit, thickness counter and thickness display units[5].

The monitor and the reference oscillators use a 6 MHz AT-cut crystal as the sensing element, because of its low temperature coefficient of frequency in the range 0–60 °C. The monitor crystal receives the evaporant inside the vacuum system and the reference crystal is located outside.

The reference and the monitor oscillators are made up of highly stable, single-chip clock generators. The long-time stability for 6 MHz crystal is 1.5 Hz variation in eight hours. The monitor oscillator is a grounded crystal configuration which enables its use in the electron beam evaporation and plasma deposition systems.

The output of the two oscillators is fed to the input of the frequency mixer. The output of the mixer is the difference of reference and monitor oscillator frequencies. The stability of the mixer for 150 KHz output frequency is 1.5 Hz variation in one hour.

Since the sampling interval generator circuit has been derived from the 6 MHz-reference oscillator, the output of the sampling interval generator is highly stable. It is used for displaying the rate and thickness of the film in angstroms by setting the density of the evaporating material.

The gating circuit generates proper control signals such as clock, reset, count input, enable, which are essential in the rate and thickness counter circuits.

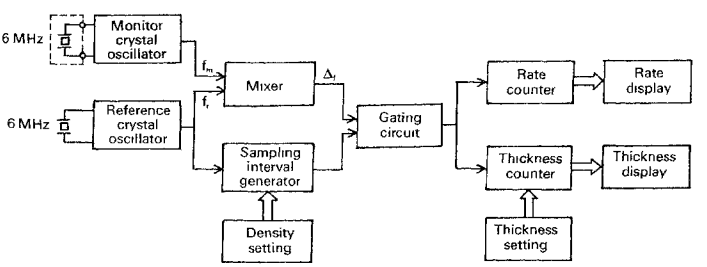

FIG. 1. Block diagram of the crystal monitor.

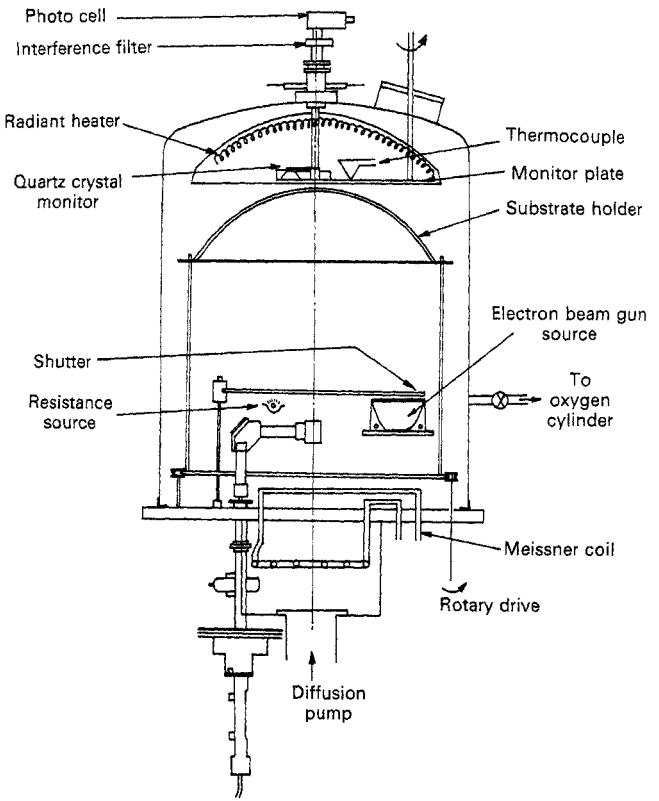

FIG. 2. Schematic diagram of vacuum deposition plant.

The rate counter is used for computing the rate of evaporation, which is determined from two consecutive samplings of the mixer output frequency. The first sampling is substracted from the second which gives the rate of evaporation which is displayed on the rate display unit.

The thickness counter is used for monitoring the total thickness of the film during evaporation. It is broadly split up into three parts comprising thickness display unit, thickness reset unit and

thickness termination unit. The thickness display unit is used for displaying the total thickness of the film. The thickness reset and termination units are used for terminating the deposition when the set value of thickness has reached.

3. Performance study

The stability and performance of the electronic subsystems of the monitor are studied separately. The overall performance of the monitor is studied by coupling it to a 20″-evaporation system which is pumped by rotary and diffusion pump combination (Fig. 2). The performance of the monitor is tested in two modes, namely, frequency and thickness modes. Different metals and dielectrics are evaporated in each mode from resistive and electron beam source at a pressure of 5×10^{-5} torr.

In the frequency mode, the performance of the monitor is tested with Edwards crystal monitor and the values are found to be quite comparable for different thicknesses. In thickness mode, by setting the density of the evaporating material, the rate and thickness are measured in angstroms. The monitor is standardised using multiple beam interferometer.

At lower thicknesses ($t < 500$ Å) the deviation in the thickness measurement is 1%, whereas at higher thicknesses it is less than 0.5%. The deviation of thickness is due to many factors like density of material, growth of deposit, rate of evaporation, smoothness of surface, etc. The deviation in thickness measurement is less in silver films because of its low stress and low acoustic losses, whereas it is more in the case of copper films because of the large stress in the films.

4. Conclusions

The monitor is highly stable, simple and comparatively inexpensive. It is used for computing the rate of evaporation and the thickness of the film in angstroms. Coating termination can be provided at a predetermined thickness. The performance of the monitor has been studied by evaporating different metals and dielectrics.

References

1. WARNER, A. W. AND STOCKBRIDGE, C. D. — A mass and thermal measurement with resonating crystalline quartz, *Vacuum microbalance techniques*, (ed.) R. F. Walker, Vol. 2, 1962, pp 71–92, Plenum.
2. STECKELMACHER, W. — Thin film monitoring techniques, in *Thin film microelectronics*, (ed.) L. Holland, 1965, pp 193, 251, Chapman and Hall.
3. LAWSON, W. H. — *J. Sci. Instrum.*, 1967, **44**, 917–921.
4. KLERK, J. AND KELLY, E. F. — *Rev. Sci. Instrum.*, 1965, **36**, 506–510.
5. SHIVALINGAPPA, L., SRINIVASAN, M. P. AND MOHAN, S. — Digital quartz crystal monitor, presented at the *National Symposium on Vaccum Technology and Analytical Instruments*, Chandigarh, Jan. 1987.